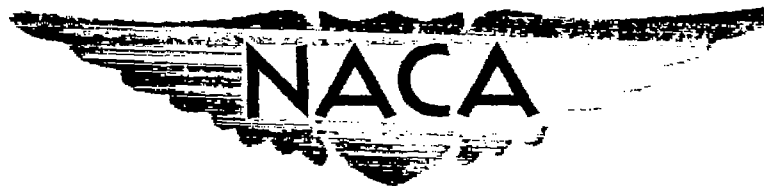


UNCLASSIFIED
~~CONFIDENTIAL~~

Copy 6
RM A50K10

NACA RM A50K10



RESEARCH MEMORANDUM

WIND-TUNNEL INVESTIGATION AT MACH NUMBERS FROM 0.50 TO 1.29 OF
AN UNSWEPT, TAPERED WING OF ASPECT RATIO 2.67 WITH LEADING-
AND TRAILING-EDGE FLAPS - LEADING-EDGE FLAPS DEFLECTED

By Louis S. Stivers, Jr., and Alexander W. Malick

Ames Aeronautical Laboratory
Moffett Field, Calif.

CLASSIFICATION CANCELLED

Authority NACA R 7 2589 Date 8/31/54

By MDA 9/14/54 See 4

CLASSIFIED DOCUMENT

This document contains classified information affecting the National Defense of the United States within the meaning of the Espionage Act, USC 50-31 and 32. Its transmission or the revelation of its contents in any manner to an unauthorized person is prohibited by law.

Information so classified may be imparted only to persons in the military and naval services of the United States, appropriate civilian officers and employees of the Federal Government who have a legitimate interest therein, and to United States citizens of known loyalty and discretion who of necessity must be informed thereof.

NATIONAL ADVISORY COMMITTEE FOR AERONAUTICS

WASHINGTON
February 26, 1951

~~CONFIDENTIAL~~

UNCLASSIFIED

NATIONAL ADVISORY COMMITTEE FOR AERONAUTICS

RESEARCH MEMORANDUM

WIND-TUNNEL INVESTIGATION AT MACH NUMBERS FROM 0.50 TO 1.29 OF
AN UNSWEPT, TAPERED WING OF ASPECT RATIO 2.67 WITH LEADING-
AND TRAILING-EDGE FLAPS - LEADING-EDGE FLAPS DEFLECTED

By Louis S. Stivers, Jr., and Alexander W. Malick

SUMMARY

Aerodynamic characteristics of an unswept wing having an aspect ratio of 2.67, a taper ratio of 0.5, and employing full-span, 25-percent chord, plain, leading-edge flaps have been determined from wind-tunnel tests of a semispan model. The data were obtained at Mach numbers from about 0.50 to 0.95 and from 1.09 to 1.29 with corresponding Reynolds numbers varying from about 0.94×10^6 to about 1.27×10^6 . Sections of the wing were uniform 0.08 chord thick from the 0.25 to the 0.75 chord points tapering to sharp leading and trailing edges. The included wedge angle of the leading and trailing edges was 18.2° . Whenever feasible the experimental results have been compared with theory.

In general, the leading-edge flap was effective in changing both the lift and pitching-moment coefficients at each angle of attack and Mach number. For the unsealed flap-wing gap configuration, however, at the highest angles of attack for the positive flap deflections the flap, in some cases, was ineffective in changing the lift coefficient and, in some instances where the incidence of the flap with respect to the free-stream direction exceeded about $\pm 10^\circ$, the flap was ineffective in changing the pitching-moment coefficient. At constant low lift coefficients the effectiveness of the leading-edge flap, compared with that of a trailing-edge flap on the same wing, was less at Mach numbers below 0.7, slightly greater at subsonic Mach numbers above 0.8, and about the same at the supersonic Mach numbers. The effects of Mach number on the rates of change of hinge-moment coefficient with angle of attack and with flap deflection were generally much larger for the leading-edge flap than for a comparable trailing-edge flap on the same wing.

INTRODUCTION

The application of leading- and trailing-edge control surfaces on low-aspect-ratio unswept wings with sharp-leading-edge airfoil sections has been proposed as a means for increasing the lift coefficients of such wings in landing or certain maneuvering attitudes, and for providing sufficient control for flight in the transonic Mach number range. Several investigations of low-aspect-ratio unswept wings employing leading- and trailing-edge control surfaces have been reported in references 1 to 6. In order to provide additional information concerning the effectiveness and hinge-moment characteristics of such control surfaces at both subsonic and supersonic Mach numbers, an investigation has been made in the Ames 1- by 3-1/2-foot high-speed wind tunnel of a semispan model of an unswept wing of aspect ratio 2.67 and taper ratio 0.5, equipped with full-span, 0.25-percent-chord, plain, leading- and trailing-edge flaps. The first part of the investigation, which was concerned with the aerodynamic characteristics of the wing employing the trailing-edge flaps, has been reported in reference 7. The present report is concerned with the aerodynamic characteristics of the wing with leading-edge flaps deflected and trailing-edge flaps undeflected. The characteristics are presented for Mach numbers from approximately 0.50 to 0.95 and from 1.09 to 1.29, with corresponding Reynolds numbers varying from about 0.94×10^6 to 1.27×10^6 . Comparisons between the experimental and calculated characteristics are made whenever practicable.

NOTATION

c chord of wing

\bar{c} mean aerodynamic chord of wing $\left(\frac{\int c^2 dy}{\int c dy} \right)$

C_D drag coefficient

C_{h_F} hinge-moment coefficient of trailing-edge flap, positive when moment tends to move trailing edge of flap downward

$$\left(\frac{\text{trailing-edge-flap hinge moment}}{2q \times \text{moment about hinge line of flap area behind hinge line}} \right)$$

C_{h_n} hinge-moment coefficient of leading-edge flap, positive when moment tends to move leading edge of flap upward

$$\left(\frac{\text{leading-edge-flap hinge moment}}{2q \times \text{moment about hinge line of flap area ahead of hinge line}} \right)$$

~~CONFIDENTIAL~~

$\frac{dC_h}{d\alpha}$	rate of change of hinge-moment coefficient with angle of attack, per degree
$\frac{dC_h}{d\delta}$	rate of change of hinge-moment coefficient with flap deflection, per degree
C_L	lift coefficient
C_m	pitching-moment coefficient about lateral axis through the quarter-chord point of the mean aerodynamic chord, with mean aerodynamic chord as reference length
$\frac{L}{D}$	lift-drag ratio
M	free-stream Mach number
q	free-stream dynamic pressure
R	Reynolds number based on mean aerodynamic chord
y	spanwise distance measured from wing-root-chord line
α	wing angle of attack, degrees
α'	wing geometric angle of attack, uncorrected for wind-tunnel jet-boundary interference (at supersonic Mach numbers, equal to α), degrees
δ_p	trailing-edge-flap deflection, measured in a plane normal to hinge line, positive when trailing edge is below chord plane
δ_n	leading-edge-flap deflection, measured in a plane normal to hinge line, positive when leading edge is above chord plane
$\frac{d\alpha}{d\delta}$	flap-effectiveness parameter, absolute value of the ratio of the change in angle of attack to change in flap deflection at a constant lift coefficient

APPARATUS

The investigation was made in the Ames 1- by 3-1/2-foot high-speed wind tunnel, a single-return closed-throat tunnel vented to the atmosphere in the return passage. The tunnel was equipped with a flexible-throat assembly (fig. 1) to permit operation at various subsonic and supersonic Mach numbers.

~~CONFIDENTIAL~~

The semispan wing model used in the investigation was the same as that employed in the investigation reported in reference 7. The model corresponded to a complete wing having an aspect ratio of 2.67, a taper ratio of 0.5, and an unswept 50-percent-chord line. The wing model was equipped with full-span, 25-percent-chord, plain, leading- and trailing-edge flaps, the hinge axes of which were coincident with the 25- and the 75-percent-chord lines of the wing. Sections of the wing in the stream-wise direction were 8-percent chord thick from the 25- to the 75-percent-chord points and tapered to sharp leading and trailing edges forming wedges with included wedge angles of 18.2° . The gaps between the flaps and the wing panel were approximately $1/32$ inch. Plan and section views of the wing together with the principal dimensions are shown in figure 2.

The wing model was mounted on an 18-inch-diameter balance plate in the tunnel sidewall, as shown in the photograph of figure 3. Approximately $1/32$ -inch gaps were maintained between the roots of the undeflected flaps and the balance plate. The face of the balance plate exposed to the tunnel air stream was flush with the tunnel wall, and an approximately $1/16$ -inch annular gap existed between the periphery of the plate and the tunnel wall. Flow through this gap from the outside atmosphere was prevented by an external pressure-tight housing. Electrical resistance strain gages were employed in measuring the force reactions on the wing and the hinge moments of the flap.

TESTS

Lift, drag, and pitching moments of the wing, and hinge moments of the leading-edge flap were determined as a function of Mach number for constant geometric angles of attack from -3° to 12° and for leading-edge flap deflections of -20° , -10° , -5° , 5° , and 10° with the flap-wing gaps unsealed. The test Mach numbers ranged from about 0.50 to 0.95 and from 1.09 to 1.29 for the wing at the smaller angles of attack with the flaps undeflected. No tests of the wing could be made at Mach numbers between 0.95 and 1.09 because of choking conditions in the tunnel test section. Lift, drag, and pitching moments corresponding to the same range of angles of attack were also obtained with the gaps sealed but only for flap deflections of -5° and 5° . For the 5° flap deflection, data for the gaps-sealed configuration were obtained only at the supersonic Mach numbers. The Reynolds numbers were based on the mean aerodynamic chord of the wing and varied from about 0.94×10^6 at a Mach number of 0.50 to a maximum of about 1.27×10^6 at a Mach number of 1.15, as shown in figure 4.

CORRECTIONS TO DATA

Wind-tunnel-wall interference corrections to the angles of attack and to the drag coefficients of the wing at subsonic Mach numbers were determined by the methods of reference 8. These corrections (additive), which are indicated in reference 9 to be independent of Mach number, are given as follows:

$$\Delta\alpha(\text{deg}) = 0.51 C_L$$

$$\Delta C_D = 0.0089 C_L^2$$

All the data corresponding to the subsonic Mach numbers have been corrected for model and wake blockage by the methods of reference 10. These blockage corrections vary with the measured drag coefficient but were generally small, never exceeding a value of 3 percent even for the highest drag coefficients.

Tare corrections determined with the wing held independently of the balance plate have been subtracted from the data at all the Mach numbers. These corrections were found to be practically independent of angle of attack or flap deflection and are given in coefficient form as follows:

<u>M</u>	<u>Lift</u>	<u>Drag</u>	<u>Pitching Moment</u>
0.50	0.018	0.031	0.006
.70	.015	.031	.004
.80	.014	.031	.003
.90	.013	.031	.001
.95	.017	.033	-.003
1.09	.001	.020	0
1.20	.005	.025	-.002
1.29	.003	.021	-.001

The pitching-moment data were obtained from the lift and drag reactions and are subject to combined errors of both the lift and drag measurements. As a consequence, the pitching-moment coefficients in the present report are regarded as being of qualitative rather than quantitative value.

At each test Mach number the stream inclination at the model position was found to be sufficiently small that no stream-angle corrections were necessary. Tunnel-wall boundary-layer measurements made at Mach numbers from 0.50 to 1.20 with the tunnel empty have indicated the existence of a turbulent boundary layer with a displacement thickness of about 0.12 inch at each Mach number. The velocity in the boundary

layer at each Mach number varied approximately as the $1/10$ power of the distance from the wall. Some drainage of low-energy air from the tunnel-wall boundary layer onto the wing may have occurred by virtue of the low induced pressures on the wing. The effect on the test data of such possible drainage, however, is unknown. It is believed that the possible flow of air around the gaps at the roots of the flaps, and through the gap between the balance plate and the tunnel wall, would have had a negligible effect on the measured data.

RESULTS AND DISCUSSION

The basic force and moment characteristics of the wing with undeflected flaps, gaps unsealed and sealed, are presented in graphical form. The corresponding characteristics for the wing with the leading-edge flaps deflected are given in tables I to V.

Lift Characteristics

Lift coefficients for the wing with flaps undeflected are shown in figure 5 as a function of Mach number with geometric angle of attack as a parameter. This figure has been reproduced from reference 7. Lift coefficients as a function of angle of attack for the various flap deflections are presented in figure 6. It is observed in this figure that the lift curves are essentially linear throughout the angle-of-attack range for Mach numbers above 0.90. In general, the effect of sealing the gaps is to increase the lift coefficients at the highest angles of attack for Mach numbers up to 0.80, but at the higher Mach numbers the effect is small.

The variation of lift coefficient with flap deflection, gaps unsealed, is shown in figure 7 for the various geometric angles of attack. It can be seen in this figure that the leading-edge flap is generally effective in changing the lift coefficient at each angle of attack and Mach number. In some cases, however, the flap is ineffective for positive flap deflections at the highest angles of attack. It is believed that there was separation of the flow from the sharp leading edge of the upward-deflected flap and that this separation caused the ineffectiveness.

The effect of Mach number on the leading-edge-flap-effectiveness parameter $dx/d\delta_n$ (evaluated for δ_n from about -5° to 5°), gaps unsealed, is shown in figure 8 for lift coefficients of 0 and 0.2 at the subsonic Mach numbers and for lift coefficients of 0, 0.2, and 0.4 at

~~CONFIDENTIAL~~

the supersonic Mach numbers. Also shown in this figure for a lift coefficient of zero are values of $da/d\delta_n$ for Mach numbers above 1.25 which were calculated using the expression for lift given in reference 11. Because of the particular geometry of the wing, the methods of this reference were applicable only for Mach numbers of 1.25 and greater. It was assumed for the calculations that the lift produced by deflection of the flap was independent of the lift produced by the incidence of the wing. As a consequence, the rate of change of lift coefficient with flap deflection was equal to the difference between the lift-curve slopes of the complete wing and that of a wing having the same plan form as the portion of the test wing behind the leading-edge flap.

In figure 8, it is observed that the effect of Mach number on the flap-effectiveness parameter $da/d\delta_n$ is relatively small throughout the ranges of Mach numbers shown. At Mach numbers between 1.25 and 1.29 it can be seen that the experimental and calculated values of $da/d\delta_n$ at zero lift are in good agreement.

Values of the trailing-edge-flap-effectiveness parameter (gaps unsealed) from reference 7 are presented in figure 9 for lift coefficients of 0 and 0.2. A comparison of the values of the flap-effectiveness parameters for the leading- and trailing-edge flaps shows that those for the leading-edge flap are less at Mach numbers below 0.7 and slightly greater at subsonic Mach numbers above 0.8. At the supersonic Mach numbers the values for both flaps are nearly the same.

Hinge-Moment Characteristics

The effect of Mach number on the hinge-moment coefficient of the undeflected leading-edge flap is shown in figure 10 for various geometric angles of attack. It is observed that the variations of hinge-moment coefficient with Mach number are relatively small, except at Mach numbers near unity, for the higher angles of attack. The asymmetry of the curves about the zero hinge-moment axis and the fact that the hinge-moment coefficients are not equal to zero at zero angle of attack are believed to be due to a slight misalignment of the flaps with the wing panel and to small errors in setting the flap-deflection angle. Although not illustrated in a figure (data given in tables I to V), the variations with Mach number of the hinge-moment coefficient for the various flap deflections at given angles of attack are somewhat greater than the variations for the undeflected flaps. No abrupt variations of hinge-moment coefficient with Mach number are generally evident in the hinge-moment data for the deflected flap.

Hinge-moment coefficients for the leading-edge flap as a function of angle of attack and of flap deflection are presented in figure 11. It is observed in this figure that the changes in the hinge-moment coefficient which accompany changes in angle of attack or flap deflection are very large, as compared with those usually noted for trailing-edge flaps. The direction of the hinge moments, for the most part, is such as to tend to increase the absolute value of the flap deflection. In general, the variations of hinge-moment coefficient with angle of attack and with flap deflection are nonlinear.

The effects of Mach number on the rates of change of hinge-moment coefficient with angle of attack and with flap deflection are shown in figure 12. Values of $dC_{h_n}/d\delta_n$ at zero angle of attack for Mach numbers above 1.25, also shown in this figure, have been calculated using the expressions for the lift and center of pressure given in reference 11 and the procedure previously described for the calculation of the flap-effectiveness parameter. It may be seen in figure 12 that the effects of Mach number on $dC_{h_n}/d\alpha$ and $dC_{h_n}/d\delta_n$ are generally large. It is also noted that the effects of flap deflection on $dC_{h_n}/d\alpha$ are large for the most part. At Mach numbers between 1.25 and 1.29 the experimental values of $dC_{h_n}/d\delta_n$ for zero angle of attack are markedly greater than those calculated.

The effects of Mach number on the rates of change of hinge-moment coefficient with angle of attack and with flap deflection for the trailing-edge flap are reproduced from reference 7 in figure 13. From a comparison of figures 12 and 13, it is observed that on the whole the effects of Mach number on $dC_h/d\alpha$ and $dC_h/d\delta$ are considerably larger for the leading-edge flap than for the trailing-edge flap.

Drag Characteristics

Drag coefficients of the wing with undeflected flaps are shown in figure 14 as a function of Mach number with geometric angle of attack as a parameter. This figure has been reproduced from reference 7. The variation of drag coefficient with lift coefficient is exhibited in figure 15 for various flap deflections. It is evident in this figure that at each Mach number large changes in the drag coefficient accompany deflections of the leading-edge flap, gaps unsealed. On the whole, sealing the gaps reduced the increments of drag coefficient due to flap deflection. A marked reduction is observed for the most part at the subsonic Mach numbers.

The reason for the apparent discrepancy between the minimum drag coefficients for the -5° and 5° flap deflections, gaps unsealed, at

several of the Mach numbers is unknown, but may possibly be attributed to a misalignment of the flap.

The variation of lift-drag ratio with lift coefficient for the various leading-edge flap deflections is presented in figure 16. It is observed in this figure that deflections of the flap do not generally provide greater lift-drag ratios at the higher lift coefficients than those for the wing with the flap undeflected. Sealing the gaps increased the lift-drag ratios for the most part. The effectiveness of the flap in improving the lift-drag ratios of the wing at the subsonic Mach numbers is much less than that indicated in reference 3 for a comparable wing (5-percent chord thick, leading- and trailing-edge angles of 5.1°) investigated at a Reynolds number of 2×10^6 . The disagreement is due largely to the differences in the increments of drag coefficient which resulted from the flap deflections. It is believed that the large drag coefficient increments of the present investigation are due to separation of the flow over the wing resulting from the effects of the low test Reynolds numbers on the particular wing section employed.

Pitching-Moment Characteristics

Pitching-moment coefficients for the wing with undeflected flaps are presented in figure 17 as a function of Mach number for various geometric angles of attack. This figure has been reproduced from reference 7. The variation of pitching-moment coefficient with lift coefficient for various flap deflections is shown in figure 18. It may be seen that the variations are generally irregular for both the subsonic and supersonic Mach numbers and do not appear to be significantly affected by sealing the gaps. In general, the rates of change of pitching-moment coefficient with lift coefficient are positive at the subsonic Mach numbers. The large positive slopes evident at these Mach numbers may be a result of the low Reynolds numbers of the investigation. At the supersonic Mach numbers the slopes are generally negative.

The variation of pitching-moment coefficient with flap deflection, gaps unsealed, for various angles of attack is presented in figure 19. It is observed that the leading-edge flap is generally very effective in changing the pitching-moment coefficient at each angle of attack and Mach number shown. In some instances, however, the flap was ineffective where the incidence of the flap with respect to the free-stream direction (i.e., $\alpha + \delta_n$) exceeded about $\pm 10^\circ$.

CONCLUSIONS

A semispan model of an unswept, tapered wing of aspect ratio 2.67 employing leading-edge flaps and having sharp leading-edge airfoil sections with a thickness-chord ratio of 0.08 has been investigated at Mach numbers from about 0.50 to 0.95 and from 1.09 to 1.29 with corresponding Reynolds numbers varying from about 0.94×10^6 to 1.27×10^6 . From the results of this investigation, the following are concluded:

1. The leading-edge flap was generally effective in producing an increment of both lift coefficient and pitching-moment coefficient at each angle of attack and Mach number. In some cases, however, for the unsealed gap configuration, the flap was ineffective in producing an increment of lift coefficient for positive flap deflections at the highest angles of attack, and ineffective in producing an increment of pitching-moment coefficient where the incidence of the flap with respect to the free-stream direction was greater than about $\pm 10^\circ$.

2. The effectiveness of the leading-edge flap at constant low lift coefficients, as compared with that of a trailing-edge flap on the same wing, was less at Mach numbers below 0.7, slightly greater at subsonic Mach numbers above 0.8, and very nearly the same at the supersonic Mach numbers.

3. On the whole, the effects of Mach number on the rates of change of hinge-moment coefficient with angle of attack and with flap deflection were much larger for the leading-edge flap than for a comparable trailing-edge flap on the same wing.

Ames Aeronautical Laboratory,
National Advisory Committee for Aeronautics,
Moffett Field, Calif.

REFERENCES

1. Lange, Roy H., and May, Ralph W., Jr.: Effect of Leading-Edge High-Lift Devices and Split Flaps on the Maximum-Lift and Lateral Characteristics of a Rectangular Wing of Aspect Ratio 3.4 With Circular-Arc Airfoil Sections at Reynolds Numbers from 2.9×10^6 to 8.4×10^6 . NACA RM L8D30, 1948.
2. Johnson, Ben H., Jr., and Bandettini, Angelo: Investigation of a Thin Wing of Aspect Ratio 4 in the Ames 12-Foot Pressure Wind Tunnel. II - The Effect of Constant-Chord Leading- and Trailing-Edge Flaps on the Low-Speed Characteristics of the Wing. NACA RM A8F15, 1948.
3. Johnson, Ben H., Jr., and Reed, Verlin D.: Investigation of a Thin Wing of Aspect Ratio 4 in the Ames 12-Foot Pressure Wind Tunnel. IV - The Effect of a Constant-Chord Leading-Edge Flap at High Subsonic Speeds. NACA RM A8K19, 1949.
4. Bandettini, Angelo, and Reed, Verlin D.: The Aerodynamic Characteristics Throughout the Subsonic Speed Range of a Thin, Sharp-Edged Horizontal Tail of Aspect Ratio 4 Equipped with a Constant-Chord Elevator. NACA RM A9E05, 1949.
5. Conner, D. William, and Mitchell, Meade H., Jr.: Control Effectiveness and Hinge-Moment Measurements at a Mach Number of 1.9 of a Nose Flap and Trailing-Edge Flap on a Highly Tapered Low-Aspect-Ratio Wing. NACA RM L8K17a, 1949.
6. Strass, H. Kurt: Free-Flight Investigation of the Rolling Effectiveness at High Subsonic, Transonic, and Supersonic Speeds of Leading-Edge and Trailing-Edge Ailerons in Conjunction with Tapered and Untapered Plan Forms. NACA RM L8E10, 1948.
7. Stivers, Louis S. Jr., and Malick, Alexander W.: Wind-Tunnel Investigation at Mach Numbers From 0.50 to 1.29 of an Unswept Tapered Wing of Aspect Ratio 2.67 With Leading- and Trailing-Edge Flaps - Trailing-Edge Flaps Deflected. NACA RM A50J09b, 1950.
8. Glauert, H.: Wind-Tunnel Interference on Wings, Bodies, and Airscrews. R.&M. No. 1566, British A.R.C., 1933.
9. Goldstein, S., and Young, A. D.: The Linear Perturbation Theory of Compressible Flow With Applications to Wind-Tunnel Interference. R.&M. No. 1909, British, A.R.C., 1943.

10. Herriot, John G.: Blockage Corrections for Three-Dimensional-Flow Closed-Throat Wind Tunnels, With Consideration of the Effect of Compressibility. NACA RM A7B28, 1947.
11. Lagerstrom, P. A., Wall, D., and Graham, M. E.: Formulas in Three-Dimensional Wing Theory. (1) Douglas Aircraft Company Rep. No. SM-11901, Aug., 1946.

TABLE I.— BASIC AERODYNAMIC DATA
 $[\delta_n = 5^\circ]$

Gaps unsealed						Gaps sealed				
M	α	C_L	C_D	C_m	C_{D_n}	M	α	C_L	C_D	C_m
0.51	-3.1	-0.096	0.038	0.007	0.051	---	---	---	---	---
.72	-3.0	-.087	.036	.008	.068	---	---	---	---	---
.82	-3.0	-.071	.040	-.003	.085	---	---	---	---	---
.88	-3.1	-.089	.049	-.004	.096	---	---	---	---	---
.91	-3.0	-.083	.061	.001	.100	---	---	---	---	---
.94	-3.0	-.087	.069	.005	.106	---	---	---	---	---
1.09	-3.0	-.113	.070	.037	.100	1.09	-3.0	-0.155	0.072	0.044
1.20	-3.0	-.123	.062	.069	.158	1.20	-3.0	-.156	.075	.048
1.29	-3.0	-.097	.076	.051	.133	1.29	-3.0	-.111	.075	.053
.51	0	.015	.032	.008	.204	---	---	---	---	---
.71	0	.029	.031	.016	.243	---	---	---	---	---
.82	0	.036	.032	.015	.280	---	---	---	---	---
.87	0	.035	.040	.025	.287	---	---	---	---	---
.91	0	.049	.045	.013	.300	---	---	---	---	---
.95	0	.067	.069	.009	.301	---	---	---	---	---
1.09	0	.064	.062	.013	.303	1.09	0	.010	.068	.057
1.20	0	.049	.070	.043	.323	1.20	0	.013	.070	.040
1.29	0	.059	.069	.034	.264	1.29	0	.046	.067	.038
.51	3.1	.161	.030	.039	.444	---	---	---	---	---
.72	3.1	.183	.033	.041	.487	---	---	---	---	---
.82	3.1	.213	.037	.040	.551	---	---	---	---	---
.87	3.1	.242	.043	.038	.550	---	---	---	---	---
.91	3.1	.254	.049	.033	.529	---	---	---	---	---
.95	3.1	.246	.078	.029	.504	---	---	---	---	---
1.09	3.0	.232	.078	.026	.469	1.09	3.0	.197	.086	.040
1.20	3.0	.212	.084	.024	.404	1.20	3.0	.184	.078	.024
1.29	3.0	.209	.077	.017	.357	---	---	---	---	---
.51	6.2	.288	.057	.033	---	---	---	---	---	---
.72	6.2	.319	.058	.039	.538	---	---	---	---	---
.83	6.2	.358	.066	.050	.681	---	---	---	---	---
.89	6.2	.386	.078	.054	.697	---	---	---	---	---
.91	6.2	.401	.089	.050	.672	---	---	---	---	---
.95	6.2	.416	.133	.035	.630	---	---	---	---	---
1.09	6.0	.393	.109	.005	.580	1.09	6.0	.396	.131	.017
1.20	6.0	.359	.113	.006	.479	1.20	6.0	.332	.200	---
1.29	6.0	.350	.107	-.006	.437	---	---	---	---	---
.51	9.2	.323	.111	.018	.485	---	---	---	---	---
.72	9.2	.361	.107	.034	.557	---	---	---	---	---
.82	9.2	.330	.117	.055	.565	---	---	---	---	---
.88	9.2	.364	.133	.059	.624	---	---	---	---	---
.91	9.3	.489	.161	.069	.804	---	---	---	---	---
.95	9.3	.595	.204	.009	.736	---	---	---	---	---
1.20	9.0	.481	.153	.002	.550	1.20	9.0	.496	.139	-.012
1.29	9.0	.482	.152	-.028	.469	---	---	---	---	---
1.20	12.0	.611	.211	-.023	.605	---	---	---	---	---
1.29	12.0	.598	.207	-.043	.525	---	---	---	---	---

TABLE II.— BASIC AERODYNAMIC DATA
 $[\delta_n = 10^\circ]$

Gaps unsealed					
M	α	C_L	C_D	C_m	C_{h_n}
0.51	-3.0	-0.052	0.058	0.041	0.283
.72	-3.0	-.016	.062	.047	.359
.82	-2.9	.029	.067	.034	.418
1.09	-3.0	-.084	.089	.070	.403
1.20	-3.0	-.075	.086	.088	.356
1.29	-3.0	-.011	.085	.010	.343
.51	0	.046	.048	.044	.403
.72	0	.065	.047	.055	.476
.82	.1	.098	.052	.055	.547
1.09	0	.104	.092	.053	.541
1.20	0	.091	.088	.063	.439
1.29	0	.118	.090	.054	.407
.51	3.1	.191	.048	.047	.511
.72	3.1	.213	.053	.056	.575
.82	3.1	.235	.061	.058	.616
1.09	3.0	.282	.130	.036	.665
1.20	3.0	.237	.103	.033	.488
1.29	3.0	.255	.108	.037	.467
.51	6.2	.305	.080	.043	.535
.72	6.2	.303	.086	.039	.569
.82	6.2	.288	.101	.049	.569
1.20	6.0	.369	.132	.022	.567
1.29	6.0	.383	.142	.009	.523
.51	9.2	.370	.117	.020	.548
.72	9.2	.330	.123	.026	.563
.83	9.1	.280	.136	.053	.560
1.20	9.0	.477	.172	.008	.642
1.29	9.0	.506	.194	-.007	.563
.51	12.2	.368	.158	.010	.526
.72	12.2	.331	.164	.030	.547
.82	12.2	.308	.182	.056	.553
1.29	12.0	.452	.214	-.285	.614



TABLE III.- BASIC AERODYNAMIC DATA
 $[\delta_n = 5^\circ]$

Gaps unsealed						Gaps sealed				
M	α	C_L	C_D	C_m	C_{m_n}	M	α	C_L	C_D	C_m
0.51	-3.1	-0.157	0.023	-0.025	-0.437	0.51	-3.1	-0.145	0.025	-0.028
.72	-3.1	-0.176	.022	-0.043	-0.496	.71	-3.1	-0.152	.021	-0.027
.82	-3.1	-0.173	.027	-0.053	-0.553	.82	-3.1	-0.170	.027	-0.031
.87	-3.1	-0.160	.032	-0.061	-0.551	.87	-3.1	-0.174	.030	-0.036
.91	-3.1	-0.177	.038	-0.059	-0.544	.91	-3.1	-0.184	.033	-0.037
.95	-3.1	-0.209	.063	-0.065	-0.523	.94	-3.1	-0.199	.047	-0.033
1.09	-3.0	-0.180	.071	-0.025	-0.383	1.09	-3.0	---	.070	---
1.20	-3.0	-0.207	---	-0.032	-0.434	1.20	-3.0	-0.228	.077	-0.018
1.29	-3.0	-0.199	.054	-0.012	-0.339	1.29	-3.0	-0.184	.073	-0.029
.51	0	-0.042	.018	-0.022	-0.293	.52	0	-0.015	.011	-0.020
.72	0	-0.045	.022	-0.026	-0.347	.72	0	-0.010	.012	-0.022
.82	0	-0.052	.026	-0.026	-0.398	.83	0	-0.011	.018	-0.021
.88	0	-0.027	.032	-0.035	-0.446	.88	0	.006	.021	-0.029
.91	0	-0.028	.037	-0.044	-0.472	.92	0	.026	.024	-0.038
.94	0	-0.069	.053	-0.031	-0.468	.95	0	-0.027	.041	-0.040
1.09	0	-0.002	.079	-0.037	-0.341	1.09	0	-0.005	.069	-0.037
1.20	0	-0.044	.068	-0.046	-0.335	1.20	0	-0.043	.066	-0.053
1.29	0	-0.042	.062	-0.032	-0.259	1.29	0	-0.035	.064	-0.046
.51	3.0	.083	.025	-0.014	-0.074	.52	3.1	.107	.013	-0.011
.72	3.0	.086	.027	-0.015	-0.125	.72	3.1	.120	.017	-0.005
.82	3.0	.073	.034	-0.005	-0.130	.82	3.1	.145	.028	-0.003
.88	3.1	.117	.043	-0.015	-0.149	.88	3.1	.182	.038	-0.017
.91	3.1	.122	.052	-0.019	-0.180	.91	3.1	.173	.043	-0.014
.94	3.1	.116	.073	-0.023	-0.209	.94	3.1	.144	.061	-0.012
1.09	3.0	.142	.091	-0.044	-0.086	1.09	3.0	.168	.078	-0.047
1.20	3.0	.104	.070	-0.051	-0.179	1.20	3.0	.116	.074	-0.050
1.29	3.0	.113	.068	-0.054	-0.158	1.29	3.0	.123	.063	-0.054
.51	6.1	.210	.039	-0.029	.038	.52	6.1	.250	.026	.009
.71	6.1	.201	.040	-0.010	.043	.72	6.1	.265	.033	.013
.81	6.1	.167	.046	.001	.048	.82	6.1	.265	.046	.018
.88	6.1	.169	.061	.016	.034	.88	6.1	.229	.060	.023
.90	6.1	.197	.068	.011	.022	.92	6.1	.241	.076	.019
.95	6.1	.284	.097	-0.021	-0.021	.95	6.2	.293	.096	-0.005
.96	6.2	.319	.119	-0.053	-0.041	1.09	6.0	.312	.098	-0.039
1.09	6.0	.296	.118	-0.056	.090	1.20	6.0	.280	.093	-0.069
1.20	6.0	.257	.094	-0.061	-0.010	1.29	6.0	.269	.090	-0.062
1.29	6.0	.258	.090	-0.061	-0.068	---	---	---	---	---
.51	9.2	.309	.067	-0.036	.342	.52	9.2	.390	.051	.016
.72	9.2	.300	.068	-0.004	.358	.72	9.2	.409	.056	.032
.82	9.1	.246	.072	.021	.351	.83	9.2	.389	.072	.037
.88	9.1	.274	.087	.028	.355	.88	9.2	.342	.085	.040
.92	9.2	.381	.114	-0.012	.343	.92	9.2	.346	.095	.036
.95	9.2	.461	.150	-0.051	.320	.96	9.3	.484	.139	.010
1.20	9.0	.408	.123	-0.067	.123	1.20	9.0	.428	.117	-0.074
1.29	9.0	.403	.117	-0.071	.065	1.29	9.0	.429	.120	-0.072
---	---	---	---	---	---	.51	12.3	.520	.097	.036
---	---	---	---	---	---	.72	12.3	.497	.115	.053
---	---	---	---	---	---	.82	12.2	.478	.138	.028
---	---	---	---	---	---	.88	12.2	.453	.181	.070
---	---	---	---	---	---	.92	12.3	.537	.228	.049
---	---	---	---	---	---	.96	12.3	.641	.303	.026
1.20	12.0	.527	.159	---	.261	1.20	12.0	.592	.153	-0.078
1.29	12.0	.547	.162	-0.074	.174	1.29	12.0	.582	.163	-0.074

TABLE IV.-- BASIC AERODYNAMIC DATA
 $[\delta_n = -10^\circ]$

Gaps unsealed					
M	α	C_L	C_D	C_m	C_{h_n}
0.51	-3.1	-0.171	0.050	-0.055	-0.593
.72	-3.1	-.184	.053	-.055	-.642
.82	-3.1	-.202	.060	-.059	-.688
1.09	-3.0	-.245	.098	-.049	-.766
1.20	-3.0	-.260	.099	-.034	-.558
1.29	-3.0	.229	.104	-.022	-.454
.51	0	-.077	.046	.184	-.518
.72	0	-.087	.047	.016	-.593
.82	-1.1	-.102	.050	.020	-.635
1.09	0	-.094	.085	-.065	-.633
1.20	0	-.133	.086	-.046	-.518
1.29	0	-.099	.089	-.061	-.431
.51	3.0	.037	.047	-.049	-.339
.72	3.0	.017	.048	-.038	-.406
.82	3.0	-.041	.056	-.023	-.461
1.09	3.0	.090	.082	-.081	-.416
1.20	3.0	.030	.082	-.087	-.437
1.29	3.0	.053	.085	-.082	-.406
.51	6.1	.149	.063	-.035	-.144
.72	6.1	.101	.066	-.022	-.162
.82	6.0	.039	.072	-.001	-.187
1.09	6.0	---	.100	-.080	-.221
1.20	6.0	.203	.102	-.095	-.416
1.29	6.0	.204	.102	-.100	-.394
.51	9.1	.190	.090	-.037	-.003
.72	9.1	.144	.093	-.016	-.005
.82	9.1	.099	.098	.015	-.004
1.09	9.0	.382	.137	-.086	---
1.20	9.0	.338	.134	-.102	-.193
1.29	9.0	.347	.129	-.100	-.243
.51	12.1	.260	.115	-.035	.134
.72	12.1	.223	.115	-.014	.139
.82	12.1	.191	.123	.014	.151
1.20	12.0	.440	.160	-.065	.037
1.29	12.0	.466	.158	-.081	-.015

TABLE V.-- BASIC AERODYNAMIC DATA
 $[\delta_n = -20^\circ]$

Gaps unsealed					
M	α	C_L	C_D	C_m	C_{h_n}
0.51	-3.1	-0.202	0.074	-0.057	-0.628
.71	-3.1	-.185	.093	-.064	-.626
.82	-3.1	-.208	.113	-.066	-.650
.87	-3.1	-.177	.126	-.047	-.678
.90	-3.1	-.198	.137	-.084	-.711
.94	-3.2	-.298	.198	-.073	-.871
.51	-.1	-.112	.061	-.053	-.591
.71	-.1	-.154	.082	-.049	-.632
.82	-.1	-.210	.096	-.049	-.648
.87	-.1	-.241	.110	-.061	-.674
.91	-.1	-.226	.133	-.036	-.742
.94	-.1	-.233	.178	-.048	-.846
.51	3.0	-.007	.066	-.078	-.605
.72	3.0	-.082	.080	-.069	-.590
.82	2.9	-.146	.092	-.061	-.586
.88	2.9	-.192	.106	-.066	-.586
.91	2.9	-.201	.123	-.070	-.634
.95	3.0	-.092	.195	-.087	-.846
.51	6.1	.094	.070	-.078	-.424
.72	6.0	.028	.082	-.076	-.491
.82	6.0	-.020	.089	-.067	-.538
.88	6.0	-.065	.098	-.066	-.560
.91	6.0	-.050	.118	-.046	-.585
.95	6.0	.107	.167	-.116	-.632
.51	9.1	.138	.097	-.108	-.368
.71	9.1	.095	.097	-.094	-.406
.82	9.0	.039	.101	-.066	-.431
.88	9.0	.044	.114	-.061	-.439
.90	9.0	.083	.127	-.074	-.456
.95	9.1	.265	.187	-.080	-.478
.52	12.1	.149	.122	-.085	-.434
.71	12.1	.128	.125	-.085	-.280
.82	12.1	.090	.129	-.060	-.311
.88	12.1	.143	.149	-.071	-.316
.90	12.1	.183	.166	-.084	-.313
.92	12.1	.258	.182	---	---
.94	12.2	.442	.246	-.136	-.335

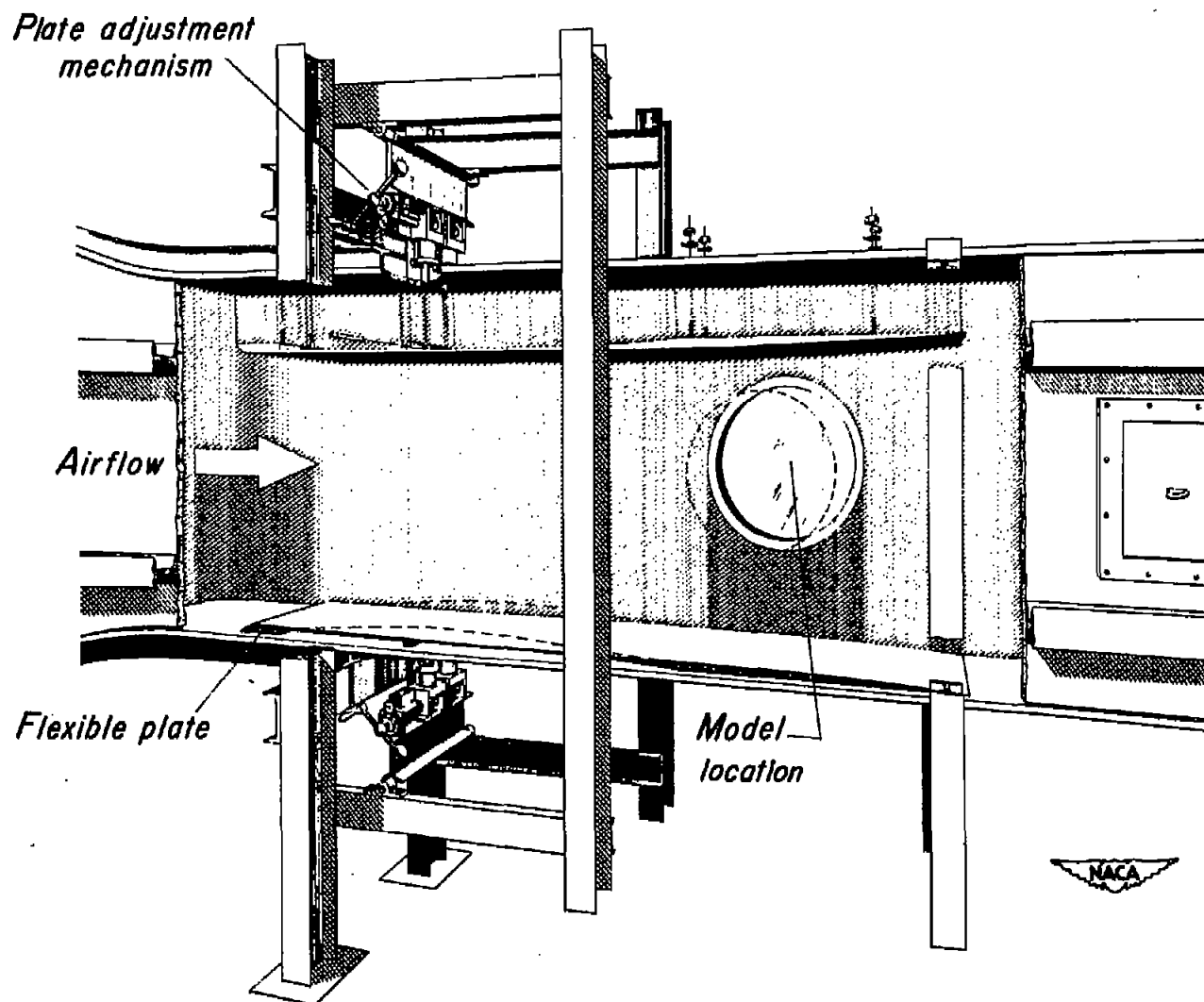


Figure 1.— Illustration of the flexible-throat mechanism in the Ames 1-by 3½-foot high-speed wind tunnel.

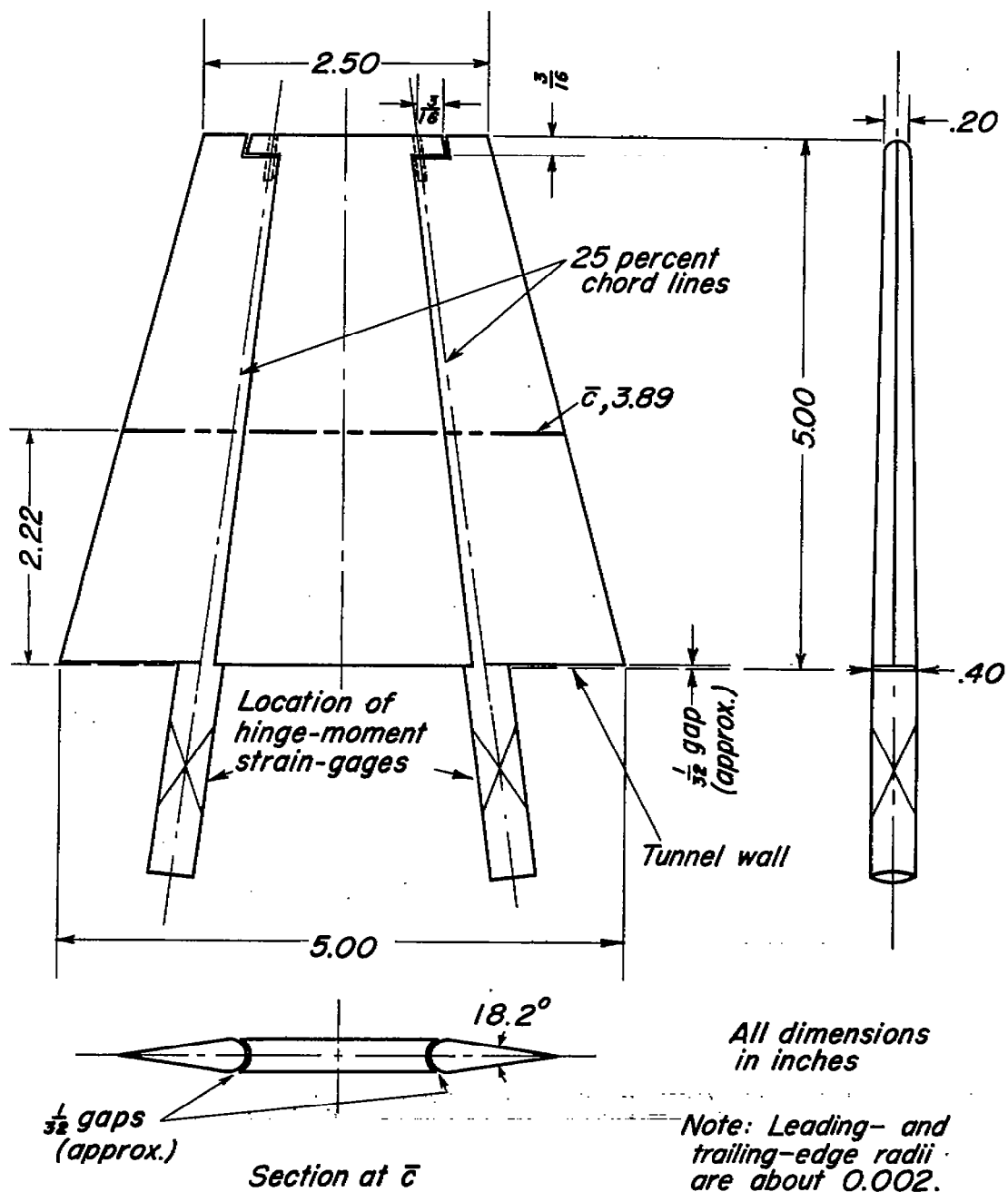


Figure 2.— Sketch of the semispan wing model with leading- and trailing-edge flaps.

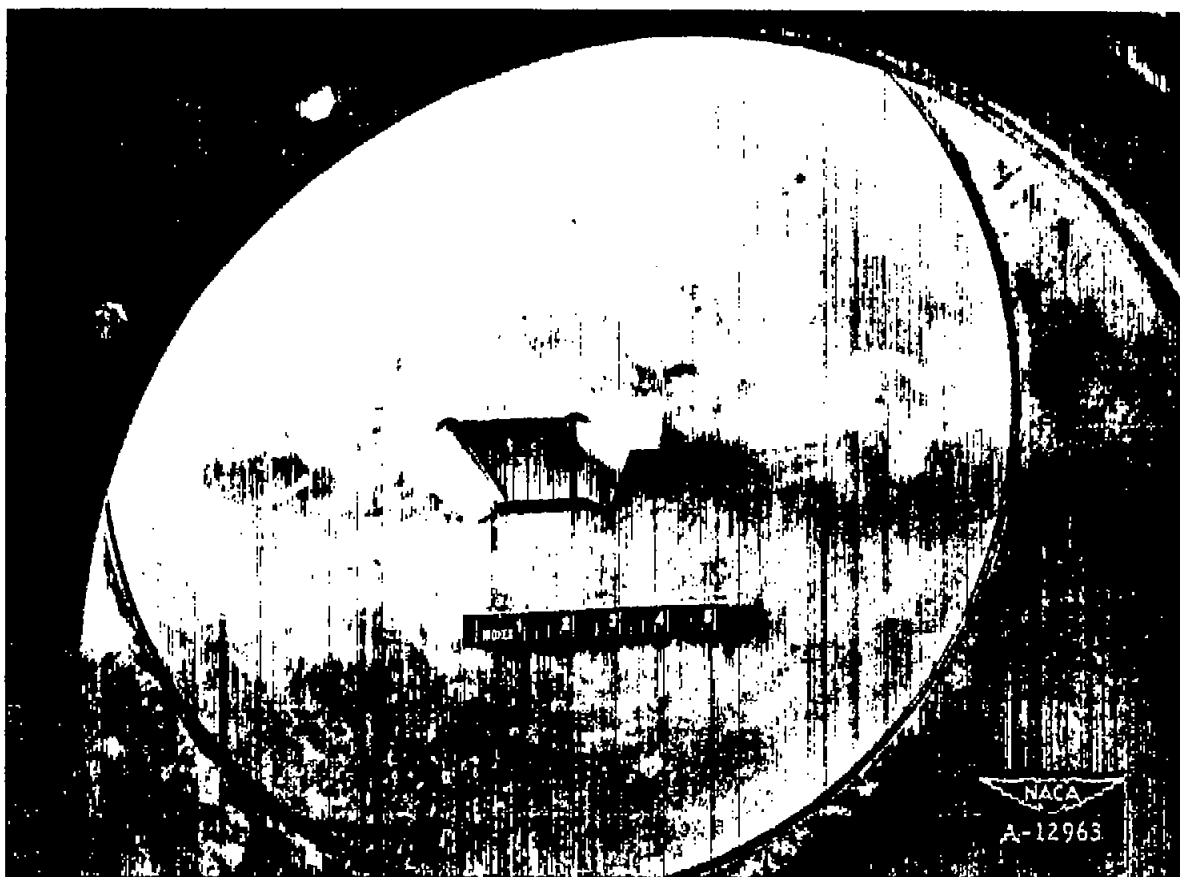


Figure 3.- Photograph of the model, with the leading- and trailing-edge flaps deflected, mounted on the semispan balance in the Ames 1- by 3-1/2-foot high-speed wind tunnel.

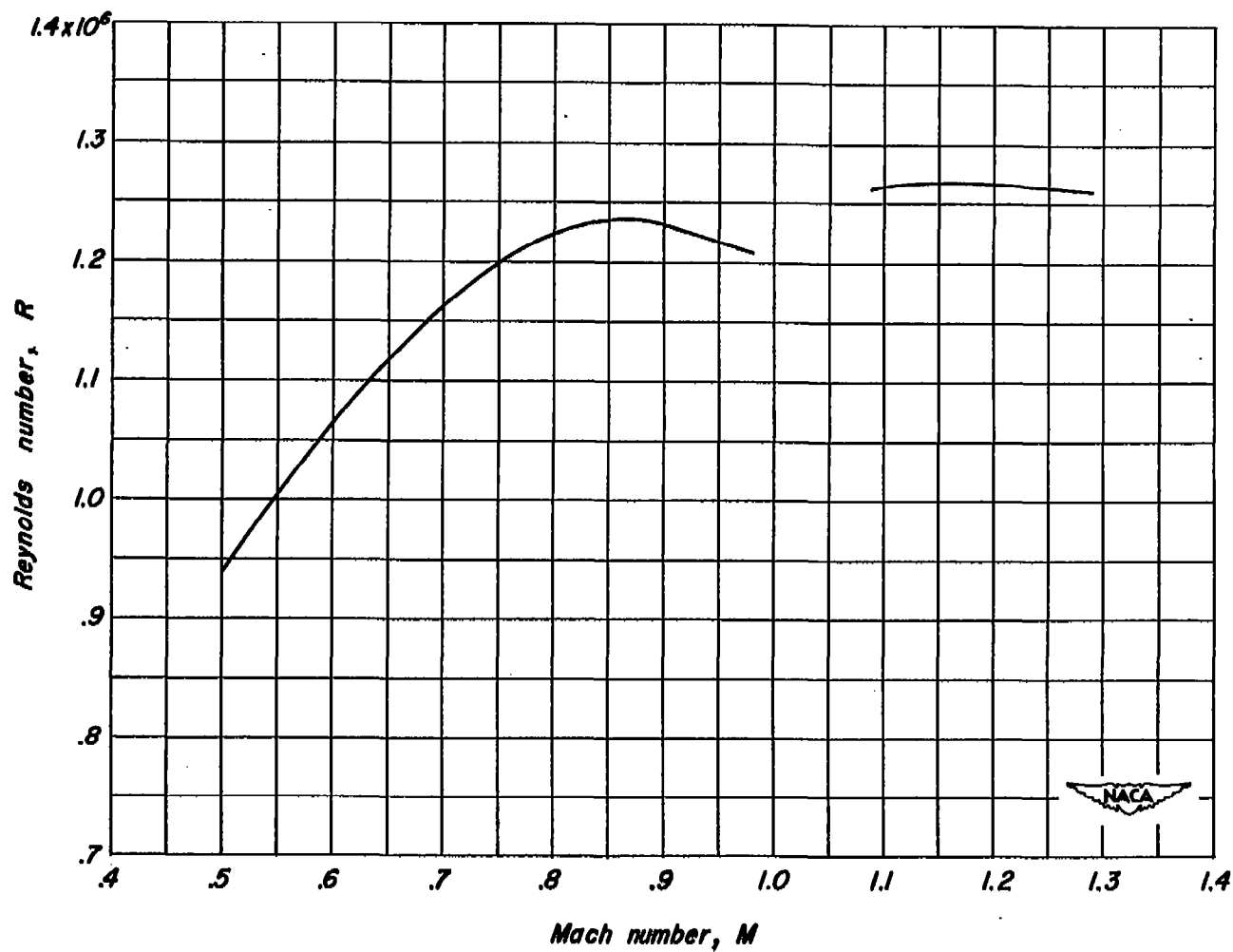


Figure 4.— Nominal variation of Reynolds number with Mach number for tests of the semispan wing of aspect ratio 2.67 in the Ames 1- by $3\frac{1}{2}$ -foot high-speed wind tunnel.

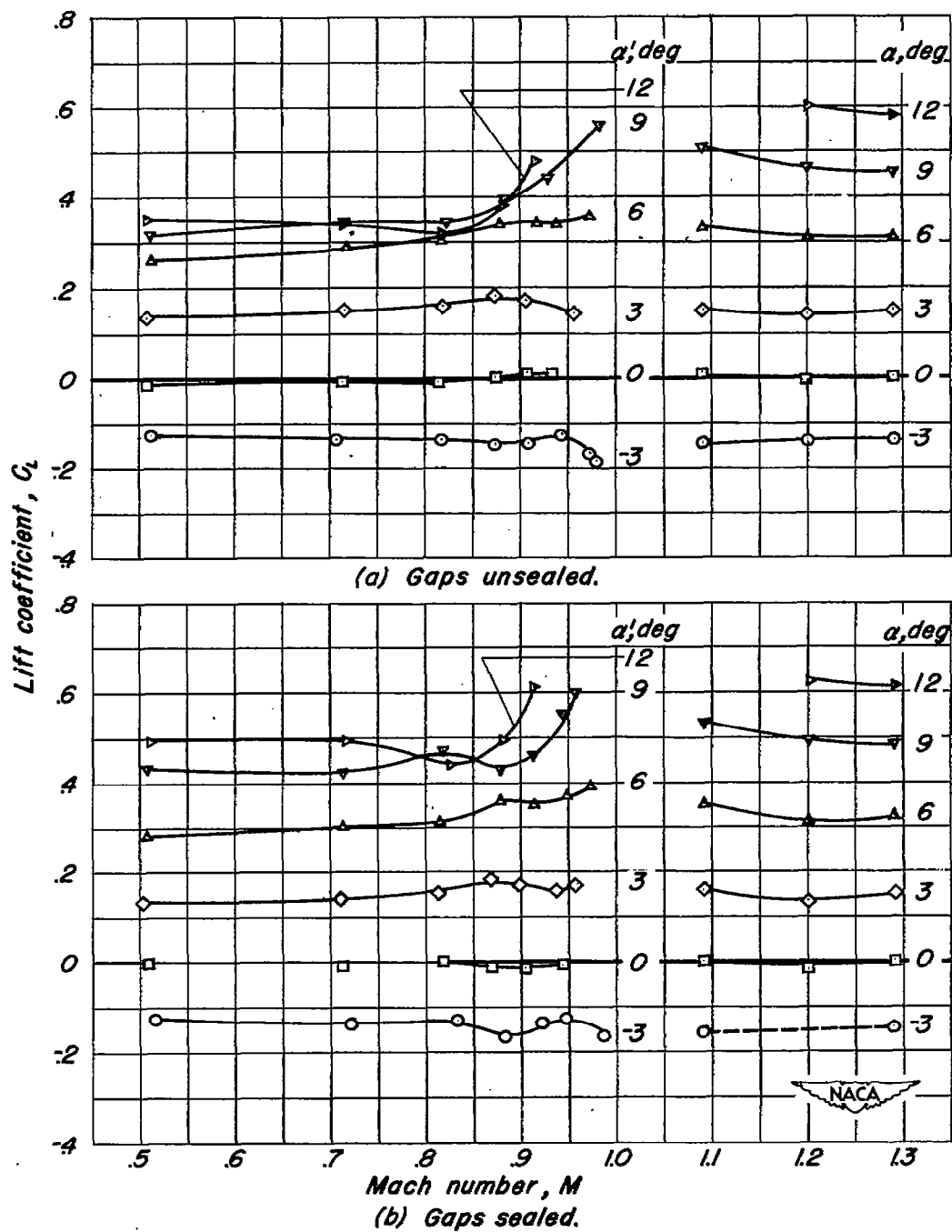


Figure 5.— Variation of lift coefficient with Mach number for various geometric angles of attack, flaps undeflected.

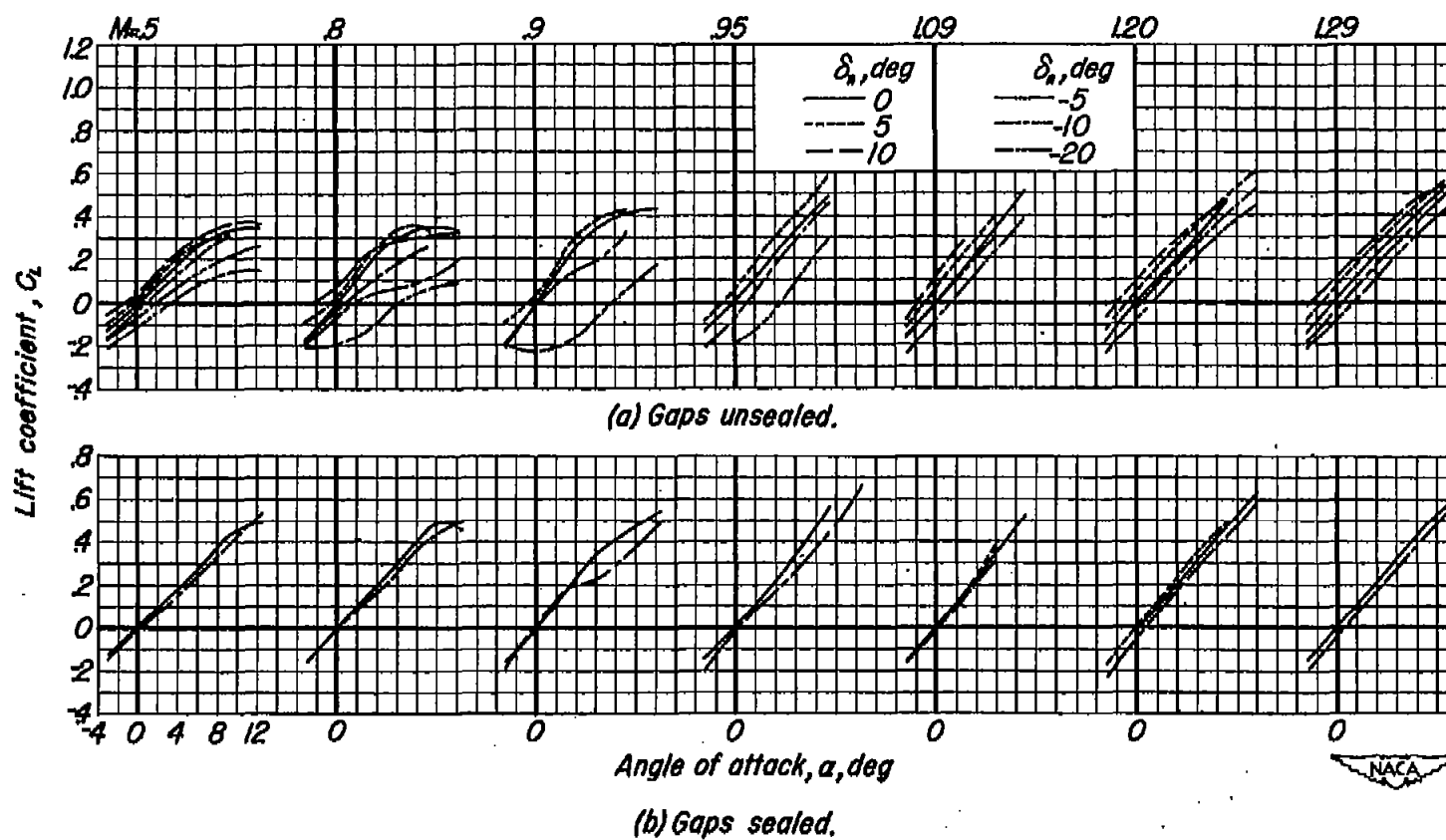


Figure 6.- Variation at several Mach numbers of lift coefficient with angle of attack for various leading-edge flap deflections.

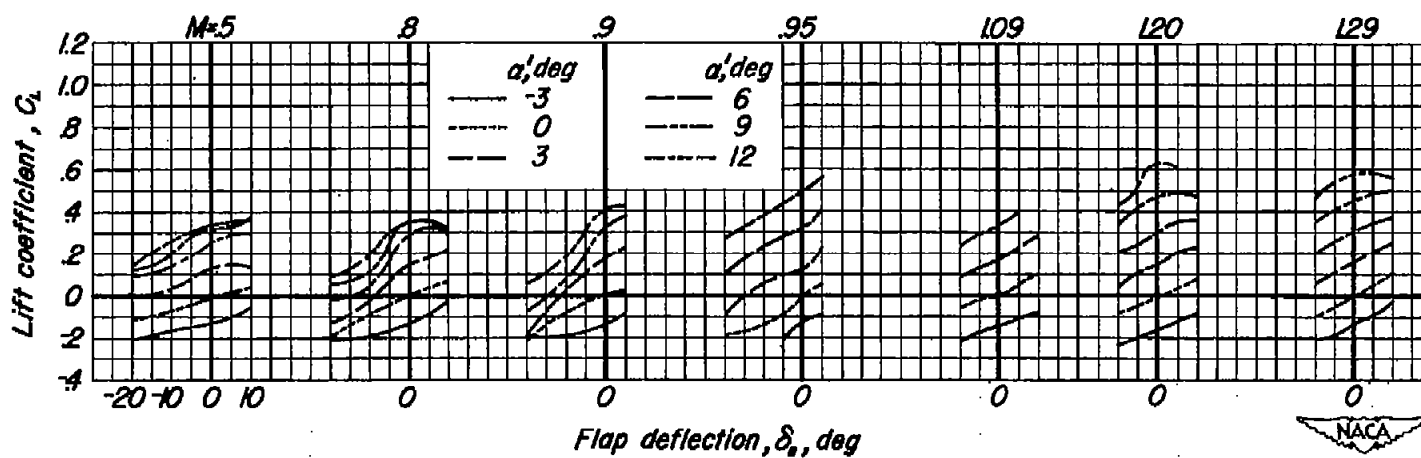


Figure 7.- Variation at several Mach numbers of lift coefficient with leading-edge flap deflection for various geometric angles of attack, gaps unsealed.

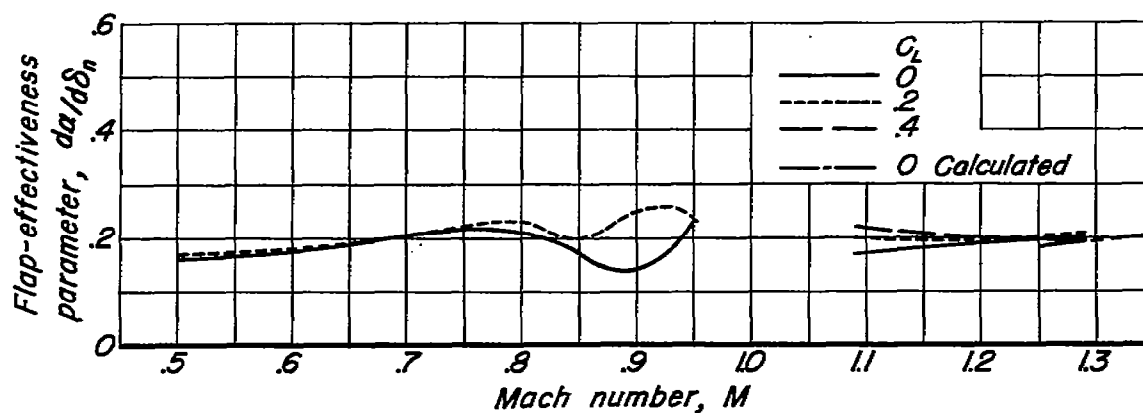


Figure 8.- Effect of Mach number on the leading-edge-flap effectiveness parameter, gaps unsealed.

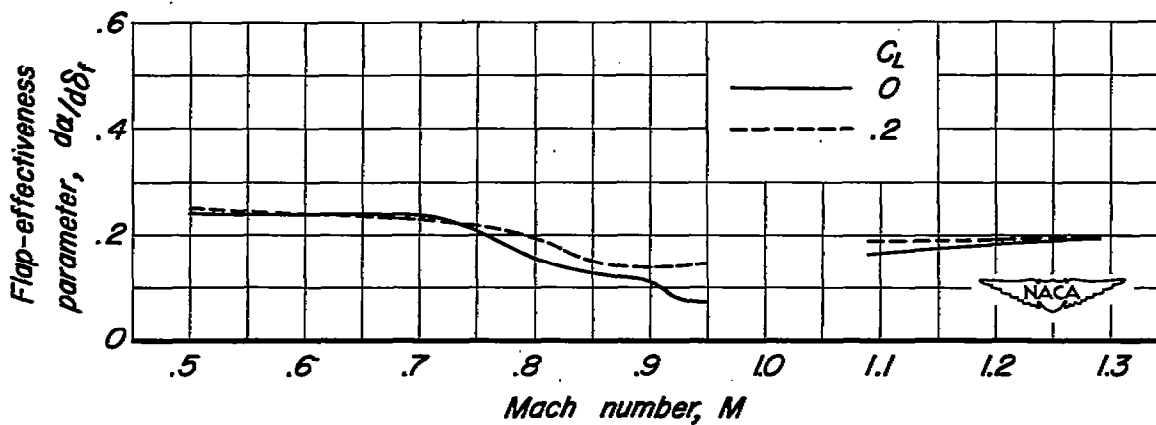


Figure 9.- Effect of Mach number on the trailing-edge-flap effectiveness parameter, gaps unsealed (data from reference 7).

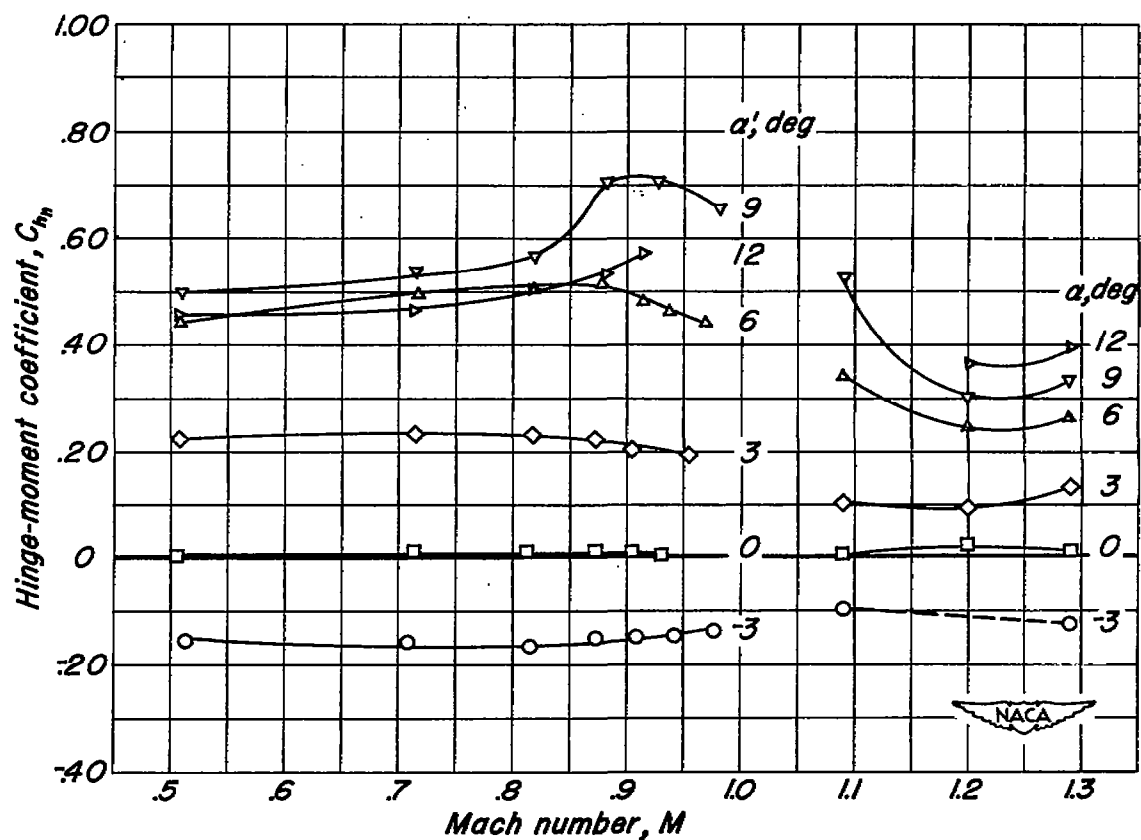
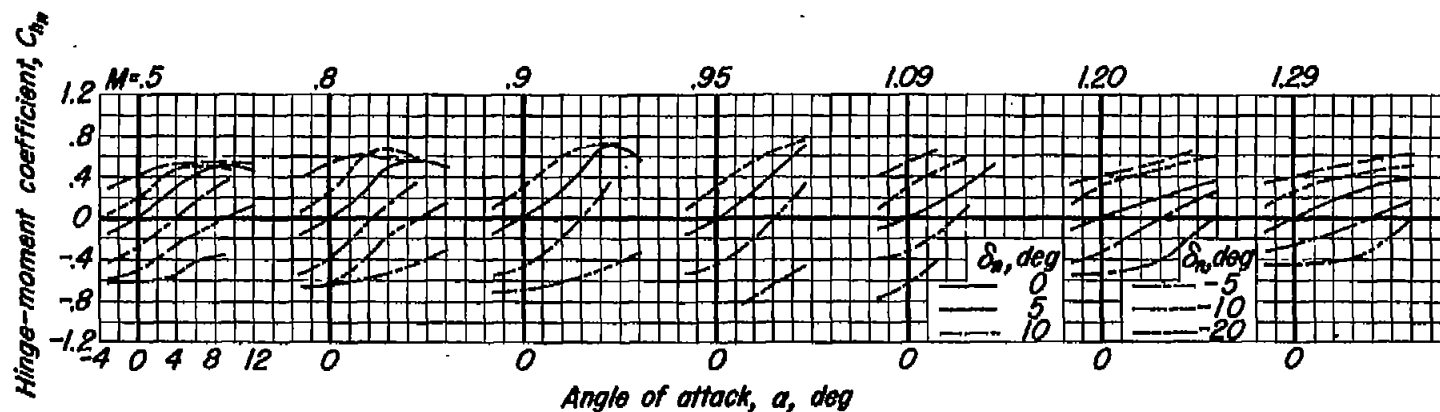
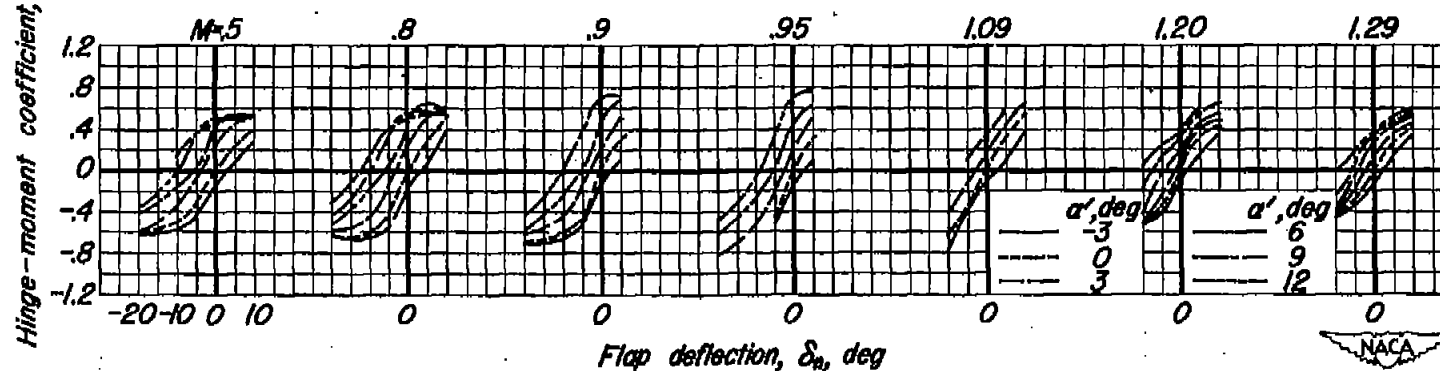


Figure 10.- Variation with Mach number of the hinge-moment coefficient of the leading-edge flap for various geometric angles of attack; flaps undeflected, gaps unsealed.

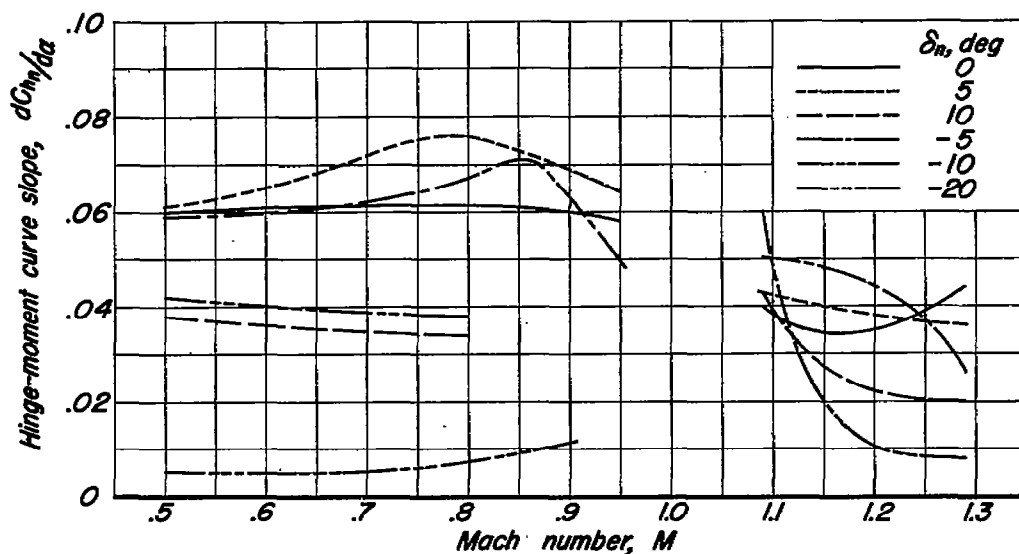


(a) Variation of hinge-moment coefficient with angle of attack for various flap deflections.

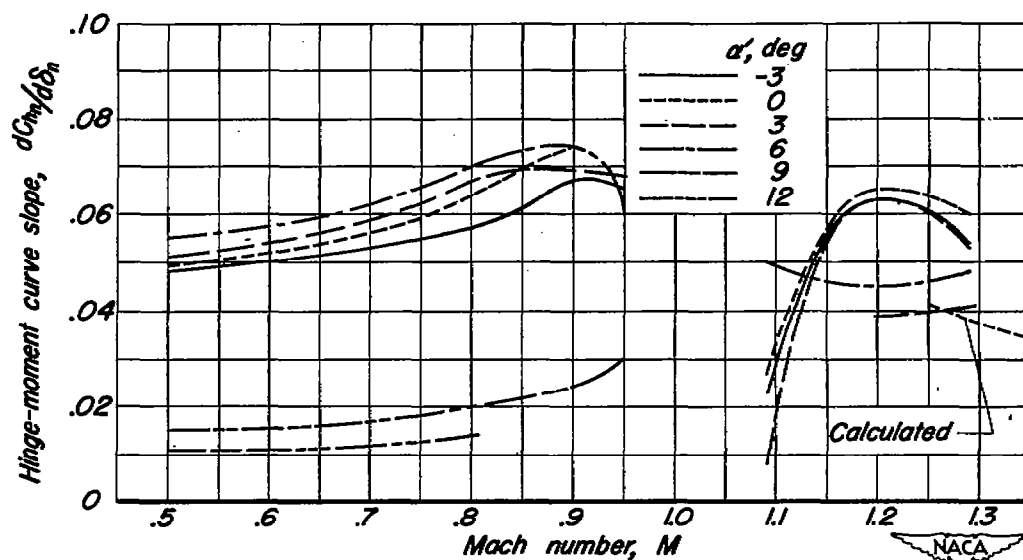


(b) Variation of hinge-moment coefficient with flap deflection for various geometric angles of attack.

Figure 11.- Variation at several Mach numbers of leading-edge flap hinge-moment coefficient with angle of attack and with flap deflection, gaps unsealed.

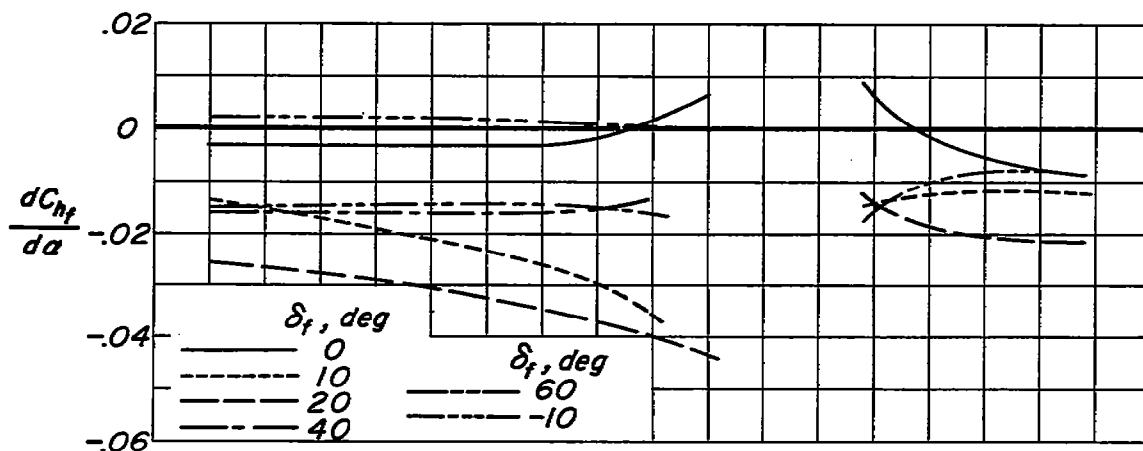


(a) Rate of change of hinge-moment coefficient with angle of attack at zero angle of attack.

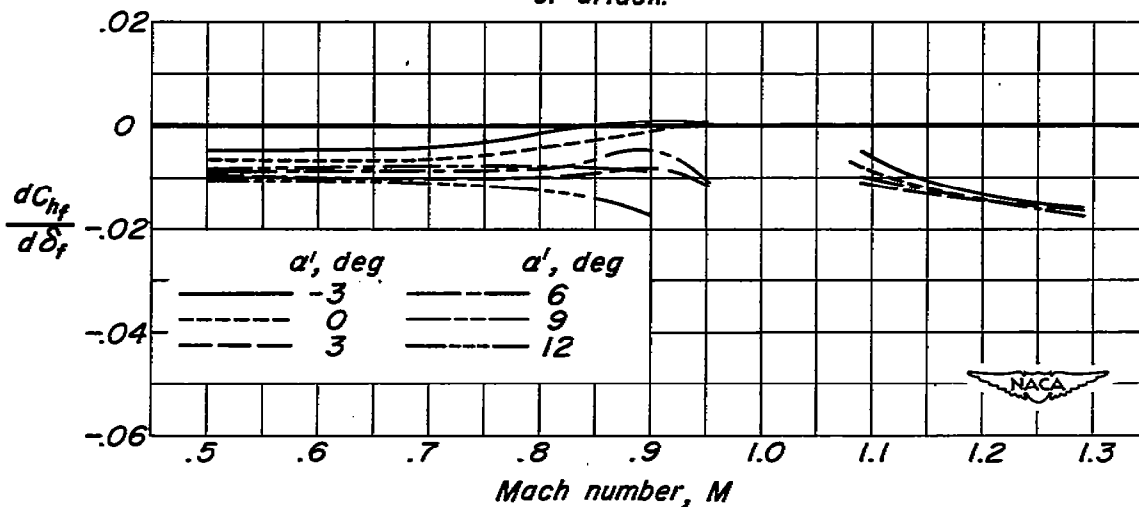


(b) Rate of change of hinge-moment coefficient with leading-edge flap deflection at 0° deflection.

Figure 12.- Effect of Mach number on the slopes of the leading-edge flap hinge-moment curves, gaps unsealed.



(a) Rate of change of hinge-moment coefficient with angle of attack at zero angle of attack.



(b) Rate of change of hinge-moment coefficient with trailing-edge flap deflection at 0° deflection.

Figure 13.— Effects of Mach number on the slopes of the trailing-edge-flap hinge-moment curves, gaps unsealed.

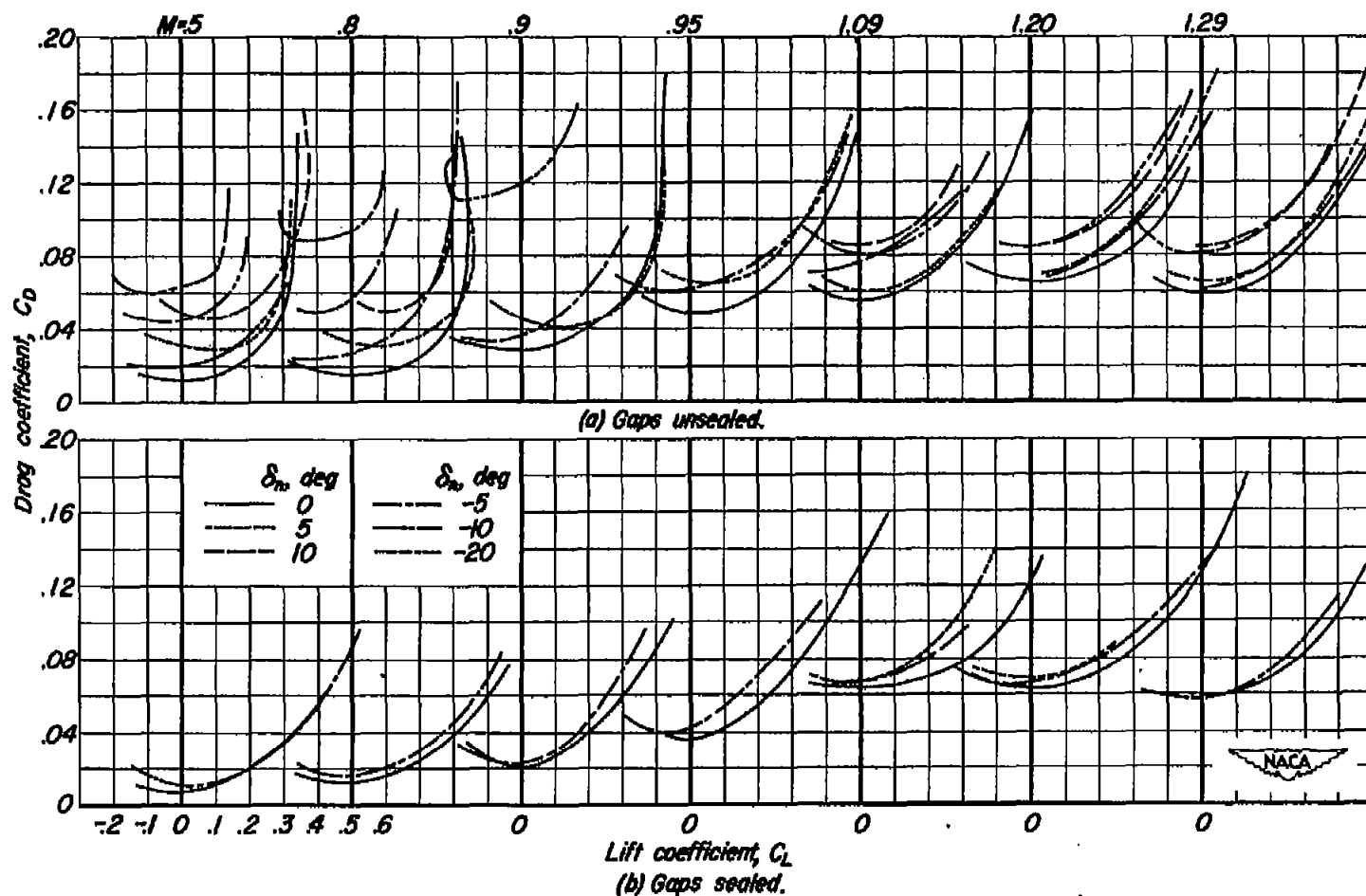


Figure 15:- Variation of drag coefficient with lift coefficient for various leading-edge flap deflections.

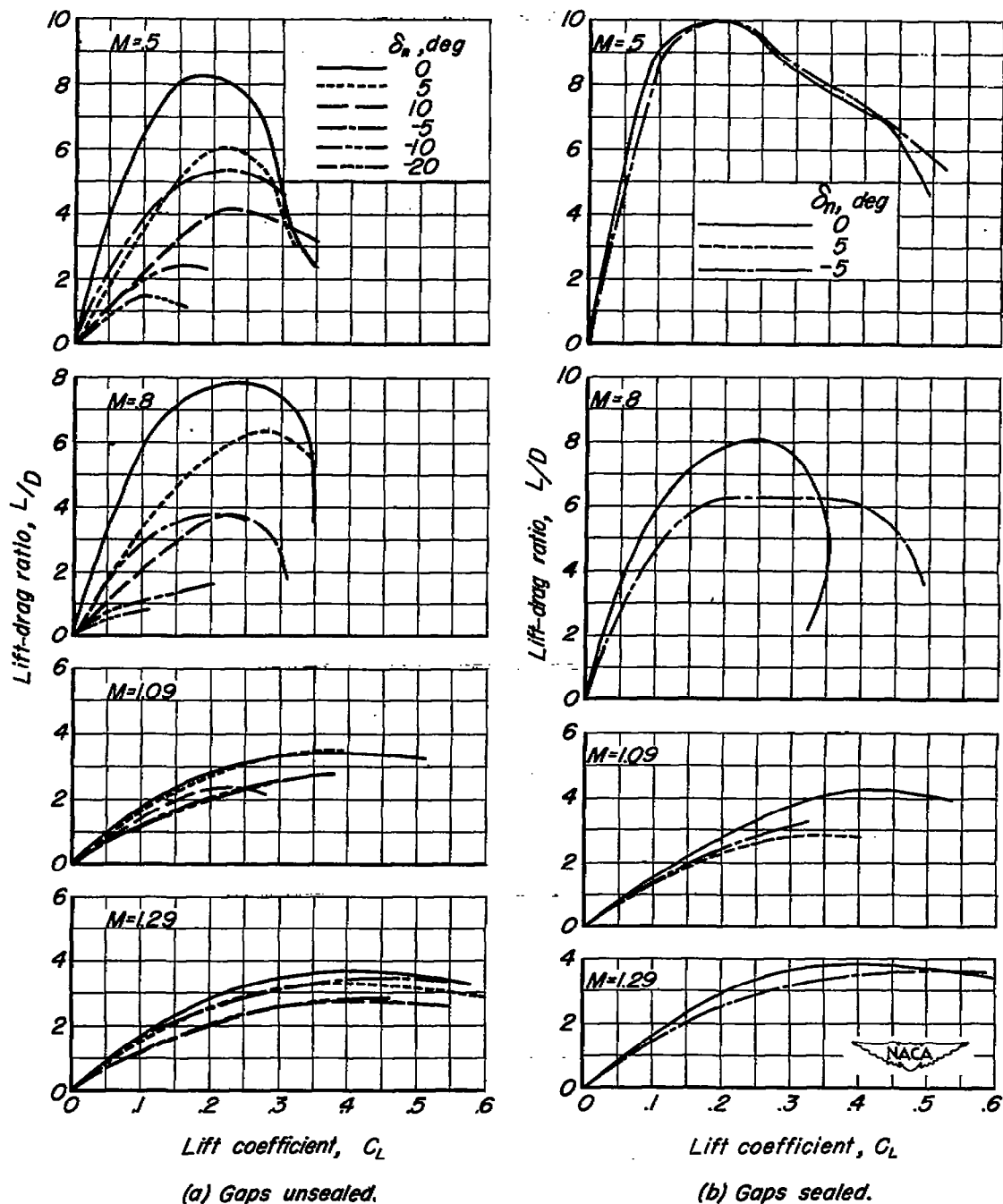


Figure 16.- Variation at several Mach numbers of lift-drag ratio with lift coefficient for various leading-edge flap deflections.

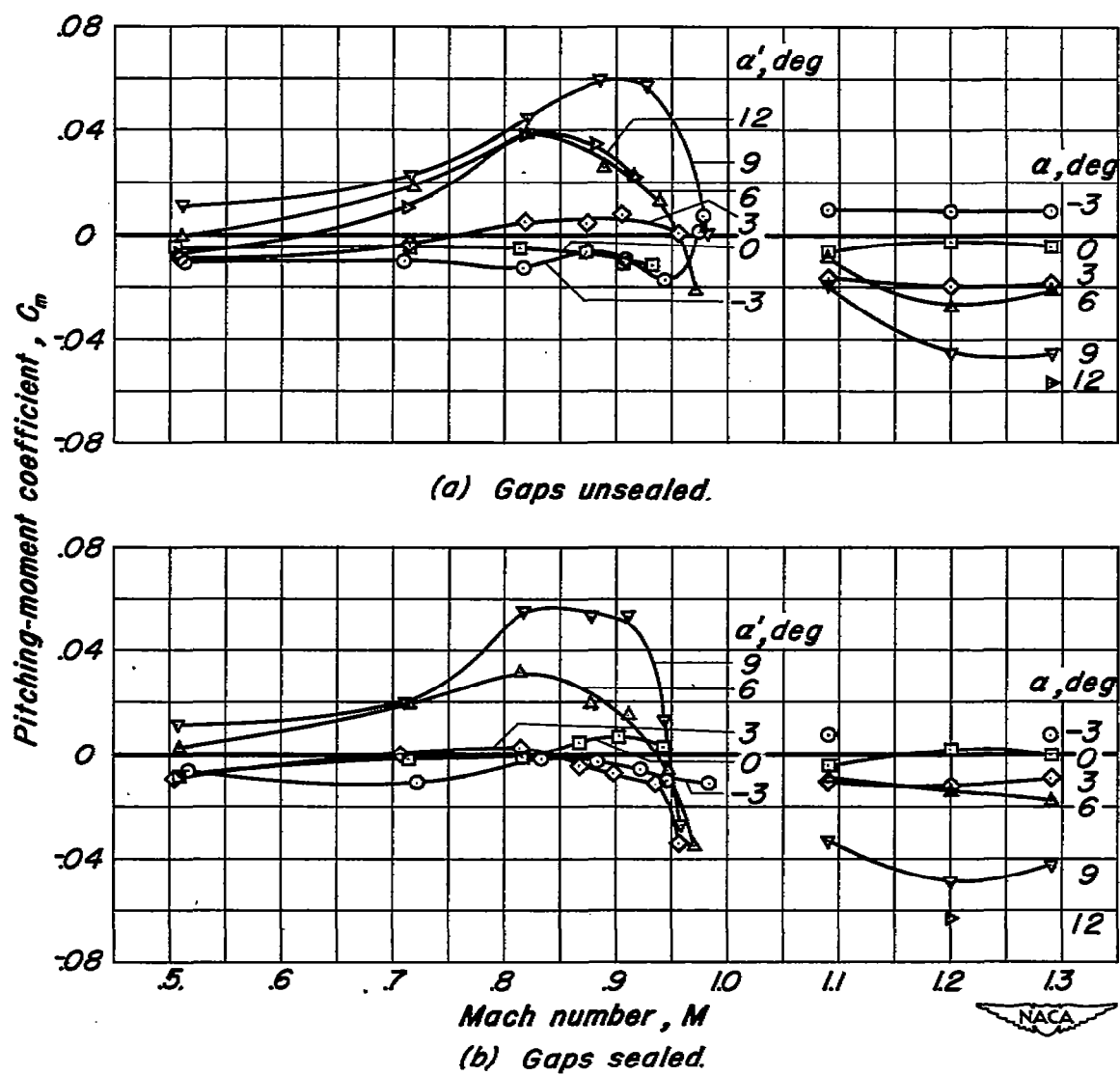


Figure 17.- Variation of pitching-moment coefficient with Mach number for various geometric angles of attack, flaps undeflected.

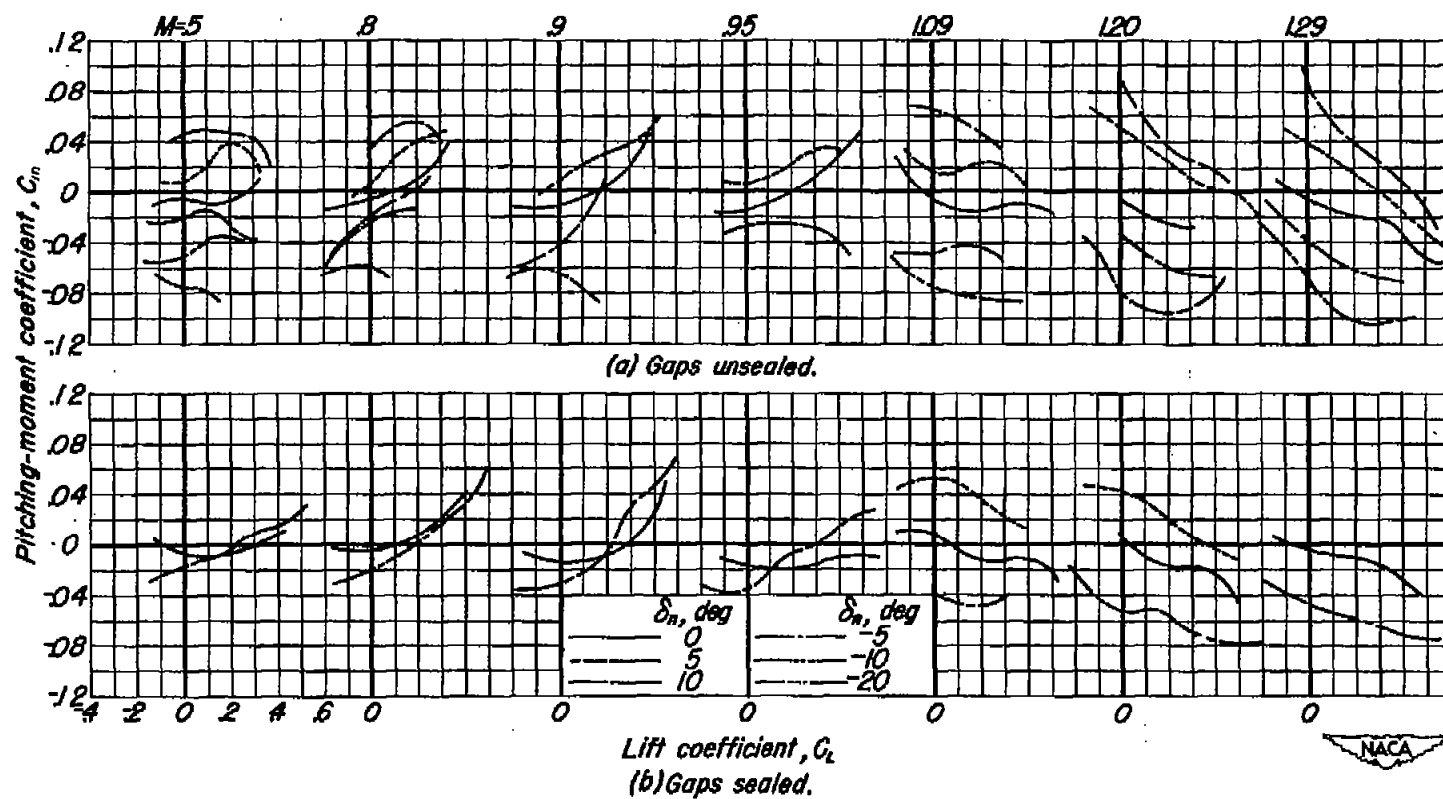


Figure 18.- Variation at several Mach numbers of pitching-moment coefficient with lift coefficient for various leading-edge flap deflections.

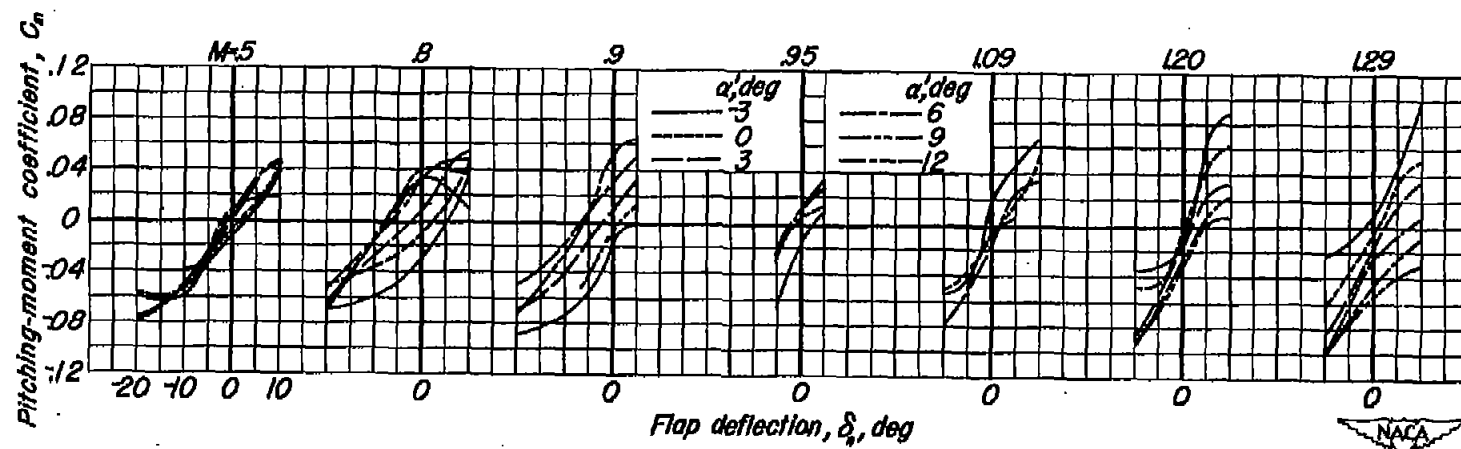


Figure 19.- Variation at several Mach numbers of pitching-moment coefficient with leading-edge flap deflection for various geometric angles of attack, gaps unsealed.

